

## Synthesis of Extremely $\pi$ -Extended Porphyrin Tapes from Hybrid *meso-meso* Linked Porphyrin Arrays: An Approach Towards the Conjugation Length

Toshiaki Ikeda, Naoki Aratani, and Atsuhiro Osuka\*<sup>[a]</sup>

**Abstract:** Directly *meso-meso*,  $\beta$ - $\beta$ ,  $\beta$ - $\beta$  triply linked porphyrin arrays are exceptional  $\pi$ -conjugated molecules exhibiting remarkably red-shifted absorption bands extending deeply in the IR region. In order to determine the effective conjugated length (ECL), we embarked on the synthesis of the porphyrin tapes far beyond the 12-mer, which is the longest we have prepared so far. In this study, to find the compromise between the feasibility of the *meso-meso* coupling reaction up to longer arrays and the sufficient solubility and chemical stability of the resultant por-

phyrin tapes, we prepared hybrid *meso-meso* linked porphyrin arrays **BOn** up to 24-mer, which have two different aryl groups, a 2,4,6-tris(3,5-di-*tert*-butyl-phenoxy) phenyl group ( $Ar^1$ ) and a 3,5-dioctyloxy phenyl group ( $Ar^2$ ). All these arrays were effectively converted into the corresponding triply linked porphyrin tapes **TBOn** by oxidation with DDQ-Sc(OTf)<sub>3</sub>. Importantly, the

low energy Q-band-like absorption bands of **TBOn** are progressively red-shifted with an increase in the number of porphyrins  $n$  until 16 but the redshift is saturated at  $n=16$ , indicating the ECL of the porphyrin tape to be around 14–16. The regularly introduced *meso*-aryl bulky substituents impose facial encumbrance, hence leading to the effective suppression of  $\pi$ - $\pi$  interactions as well as improvement of the chemical stabilities of **TBOn**.

**Keywords:** conjugation • molecular wires • oligomerization • porphyrin tapes • porphyrinoids

### Introduction

Organic molecules with extended  $\pi$ -conjugated systems have attracted considerable interest because of their possible applications to organic conducting materials, non-linear optical (NLO) materials, near-infrared (NIR) dyes, and molecular wires.<sup>[1–3]</sup> Therefore, extensive synthetic efforts have been made towards such conjugated molecular systems but have often encountered serious problems such as synthetic difficulty, chemical instability, and poor solubility with increasing the size of  $\pi$ -conjugated systems. For the use of these extended  $\pi$ -conjugated systems to electronic and optical devices, such problems need to be solved. In this respect, discrete molecules with extended  $\pi$ -conjugation should be equipped with chemical stability and good solubility. Addi-

tionally, for one-dimensional  $\pi$ -systems, there is an intrinsic problem of saturation as characterized by the effective conjugated length (ECL). ECL defines the extent of  $\pi$ -conjugated systems in which the electronic delocalization is limited and at which point the optical, electrochemical, and other physical properties reach a saturation level that is common with the analogous polymer.<sup>[1a,3c]</sup>

Porphyrin, a tetrapyrrolic pigment with an 18 $\pi$ -electron conjugated system, has been used in a variety of fields including reaction catalyst, artificial photosynthesis, photodynamic therapy, sensors, and so on.<sup>[4]</sup> Electronic properties of porphyrins are susceptible to chemical modifications at the periphery. These characteristics have been used, through the attachments of unsaturated segments to a porphyrinic  $\pi$ -network, to create conjugated porphyrins that exhibit rather altered optical and electrochemical properties.<sup>[5–12]</sup> To extend the  $\pi$ -conjugation of porphyrin oligomers, it is important to enforce a planar structure by installing multiple direct linkages between the porphyrin moieties. Along with this strategy, we have recently explored directly *meso-meso*,  $\beta$ - $\beta$ ,  $\beta$ - $\beta$  triply linked porphyrin arrays that are so-called as porphyrin tapes. These porphyrin arrays are unprecedented in respect of the extent of  $\pi$ -conjugation, in that their absorption spectra exhibits the progressive red-shift, reaching an exception-

[a] Dr. T. Ikeda, Dr. N. Aratani, Prof. Dr. A. Osuka

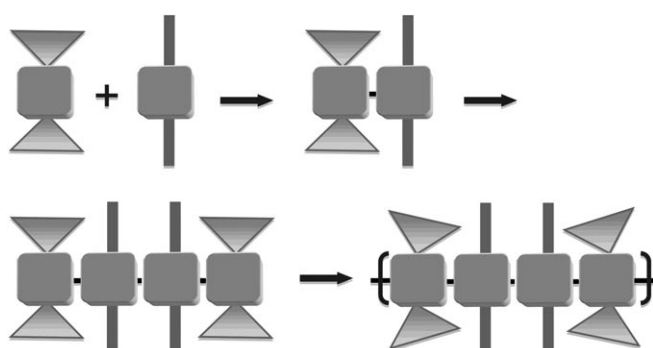
Department of Chemistry  
Graduate School of Science  
Kyoto University  
Kitashirakawaoiwake-cho, Sakyo-ku, Kyoto 606-8502 (Japan)  
Fax: (+81) 75-753-3970  
E-mail: osuka@kuchem.kyoto-u.ac.jp

 Supporting information for this article is available on the WWW under <http://dx.doi.org/10.1002/asia.200900125>.

ally red-shifted absorption band at 2800 nm for the dodecameric porphyrin tape **1a** (Figure 1).<sup>[13]</sup> These features are quite intriguing, since they do not exhibit a saturation behavior up to the dodecamer, indicating that ECL of these arrays is at least larger than 12. Additionally, these porphyrin tapes have been also shown to be promising as nonlinear optical materials, as recent studies revealed their exceptionally large two-photon absorption (TPA) values.<sup>[14,15]</sup>

Despite these promises, triply linked porphyrin tapes have serious problems such as poor solubility, strong stacking tendency, and chemical instability, all of which become more serious with increasing number of porphyrin units. In order to solve these problems, we prepared doubly-strapped porphyrin tapes<sup>[16]</sup> and insulated porphyrin tapes by bulky *meso*-aryl substituents.<sup>[17]</sup> These porphyrin tapes were synthesized up to dodecamer **1b** and tetramer **1c**, respectively. Chemical instability was certainly improved in the doubly-strapped porphyrin tapes but their solubility became seriously dropped upon an increase in the number of the array. Both the chemical stability and solubility were considerably improved in the insulated porphyrin tapes, but the *meso*-*meso* coupling reactions became increasingly difficult for longer arrays, probably as a consequence of a continuous buttressing effect. Accordingly, the longest array in the latter series is the tetramer **1c** and we could not find any suitable conditions for the coupling of **1c**.

In the present study, to overcome these problems, we employed the hybrid strategy to use, as a construction motif, a *meso*-*meso* linked tetraporphyrin unit that consists of two terminal porphyrins, bearing bulky *meso*-aryl substituents, and two internal porphyrins, bearing soluble long *meso*-aryl substituents (Scheme 1). The idea is to provide substantial facial encumbrance against  $\pi$ - $\pi$  stacking yet provide suffi-



Scheme 1. Schematic representation for making hybrid porphyrin arrays. The triangle shows  $\text{Ar}^1$  and the stick shows  $\text{Ar}^2$ .

cient space to mitigate the serious steric buttressing effect for further coupling. In this paper, we report the synthesis of a new series of hybrid porphyrin arrays, which have 2,4,6-tris(3,5-di-*tert*-butylphenoxy)phenyl group ( $\text{Ar}^1$ ) and 3,5-dioctyloxyphenyl group ( $\text{Ar}^2$ ).

## Results and Discussion

### Synthesis of *meso*-*meso* Linked Porphyrins

*Meso*-*meso* linked hybrid diporphyrin **BO2** was synthesized as shown in Scheme 2. Mono *meso*-borylated  $\text{Zn}^{II}$  porphyrin with  $\text{Ar}^1$  (**BB1**) and mono *meso*-bromo porphyrin with  $\text{Ar}^2$  (**BrO1**) were synthesized following the reported methods.<sup>[18]</sup> Suzuki–Miyaura cross coupling reactions of usual porphyrins have been already developed with satisfactory yields.<sup>[19]</sup> In contrast, the Suzuki–Miyaura coupling reaction of **BB1** and **BrO1** ( $\text{Cs}_2\text{CO}_3$ ,  $\text{Pd}(\text{PPh}_3)_4$ , toluene/DMF (2:1)) and follow-

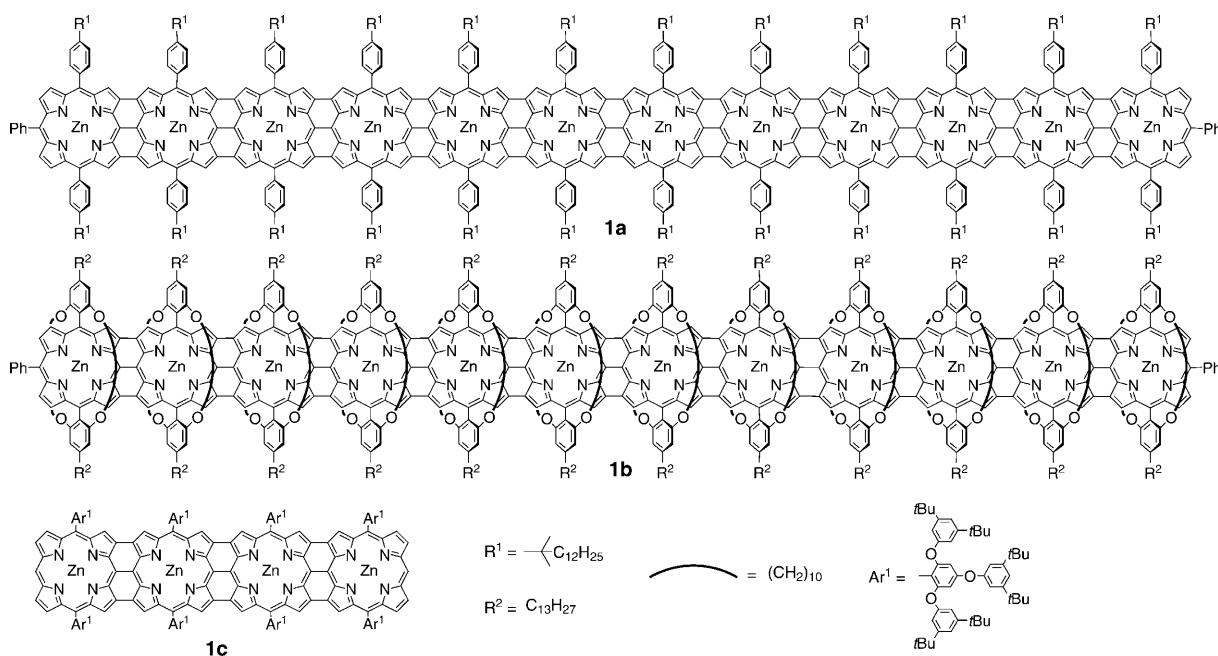
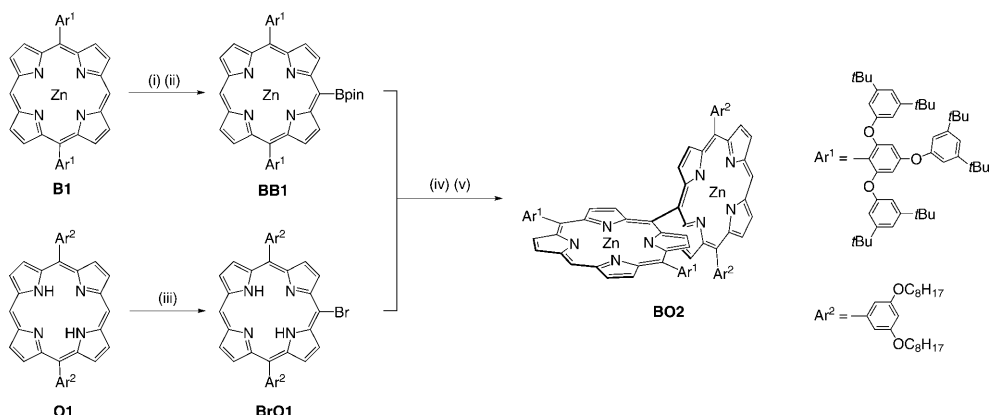


Figure 1. Molecular structures of **1a**, **1b**, and **1c**



**Scheme 2.** Synthesis of **BO2**. (i) NBS (1.1 equiv), pyridine, CHCl<sub>3</sub>. (ii) pinacolborane, PdCl<sub>2</sub>(PPh<sub>3</sub>)<sub>2</sub>, triethylamine, 1,2-dichloroethane, 62 % for 2 steps. (iii) NBS (1.1 equiv), pyridine, CHCl<sub>3</sub>, 53 %. (iv) Pd<sub>2</sub>(dba)<sub>3</sub>, tri-2-furylphosphine, Cs<sub>2</sub>CO<sub>3</sub>, CsF, THF, DMF, H<sub>2</sub>O. (v) Zn(OAc)<sub>2</sub>, methanol, CHCl<sub>3</sub>, 23 % for 2 steps.

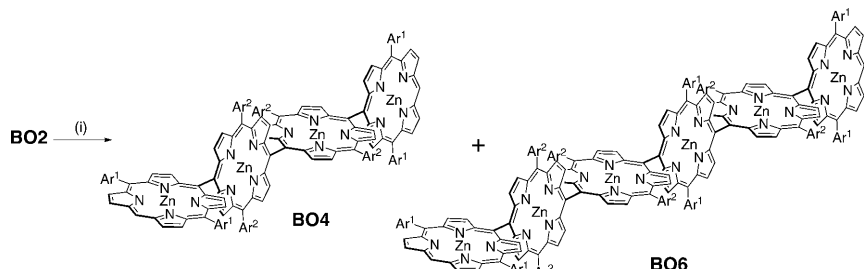
ing zinc(II) insertion, gave *meso*-*meso* linked hybrid diporphyrin **BO2** in only 9% yield. The poor yield may be ascribed mainly to the severe steric hindrance of Ar<sup>1</sup>. The yield was improved up to 23% by using tri-2-furylphosphine instead of triphenylphosphine and THF/DMF/H<sub>2</sub>O (10:2:1) as solvent. Diporphyrin **BO2** exhibited the parent molecular ion peak at *m/z*=2782.31 (calcd for C<sub>180</sub>H<sub>222</sub>N<sub>8</sub>O<sub>10</sub>Zn<sub>2</sub>, 2783.57) in the MALDI-TOF mass spectrum. The 600 MHz <sup>1</sup>H NMR spectrum of **BO2** in CDCl<sub>3</sub> exhibited two singlet peaks for *meso* protons at 10.39 and 10.23 ppm, four sets of mutually coupled doublets for the peripheral β-protons at 9.50 and 9.27 ppm, 9.47 and 9.44 ppm, 8.95 and 8.07 ppm, and 8.73 and 8.09 ppm in line with the assigned *meso*-*meso* linked hetero porphyrin dimer structure (see Figure S1 in the Supporting Information).

The silver(I)-promoted *meso*-*meso* coupling reaction is seriously influenced by steric hindrance of the *meso*-aryl substituent.<sup>[17]</sup> Reflecting this trend, *meso*-*meso* linked porphyrin tetramer **BO4** was formed as a result of regioselective coupling of **BO2** at the Ar<sup>2</sup> side in 35% yield under mild conditions (3 equivalent of AgPF<sub>6</sub> at room temperature for 12 h) along with recovered **BO2** (56%). A trace amount of *meso*-*meso* linked porphyrin hexamer **BO6** was also obtained as a byproduct in this reaction, as a result of further coupling of **BO4** and **BO2** (Scheme 3). These two oligomers were characterized by <sup>1</sup>H NMR, MALDI-TOF mass, and UV/Vis absorption spectroscopy.

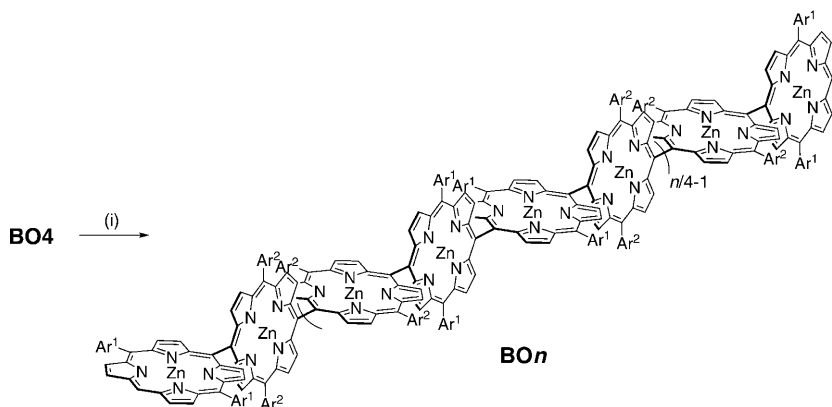
UV/Vis absorption spectroscopy. Each compound exhibited the expected parent molecular ion peaks in the MALDI-TOF mass spectroscopy. The <sup>1</sup>H NMR spectrum of **BO4** in CDCl<sub>3</sub> provided a singlet at 10.23 ppm for the *meso* proton, and four sets of mutually coupled doublets for the β-protons at 9.48 and 9.45 ppm, 9.03 and 8.24 ppm, 8.89 and 8.32 ppm, and 8.75 and 8.13 ppm, which indicates **BO4** has S<sub>4</sub> symmetry.

Under the same mild conditions, *meso*-*meso* coupling reaction of **BO4** did not proceed at all, probably arising from the steric hindrance at the edge porphyrins that bear large Ar<sup>1</sup> substituents. We, thus, attempted the coupling reaction of **BO4** under stronger conditions (Scheme 4). Coupling products **BO8** (9%) and **BO12** (2%) were obtained when **BO4** was refluxed with 10 equivalents of AgPF<sub>6</sub> in CHCl<sub>3</sub> for 72 h. Coupling yields were further improved by the addition of *N,N*-dimethylacetamide (DMA) (1 mol %),<sup>[21]</sup> which gave **BO8** (15%), **BO12** (5%), **BO16** (2%), 20-mer (1%), and 24-mer (trace). These oligomers were all separated in a pure form and fully characterized by <sup>1</sup>H NMR, MALDI-TOF mass, and UV/Vis absorption spectroscopy. MALDI-TOF mass spectrometry was very effective for the detection of the parent molecular ion peaks of these oligomers. The <sup>1</sup>H NMR spectra of these oligomers in CDCl<sub>3</sub> provided a singlet around 10.2 ppm for the end *meso*-protons, and several peaks of doublets from 8.1 to 9.5 ppm for the β-protons, which indicates these oligomers also have S<sub>4</sub> symmetry.

In the <sup>1</sup>H NMR spectra of 20-mer and 24-mer, some minor peaks were observed after purification by silica-gel column chromatography and recrystallization, and the UV/Vis absorption spectra of these compounds showed additional peaks around 700 to 1700 nm, which are attributed to triply linked porphyrin dimer and trimer (see Supporting In-



**Scheme 3.** Ag<sup>I</sup>-promoted oxidation coupling of **BO2**. (i) AgPF<sub>6</sub> (3 equiv), CH<sub>3</sub>CN, CHCl<sub>3</sub>, room temperature, 12 h.

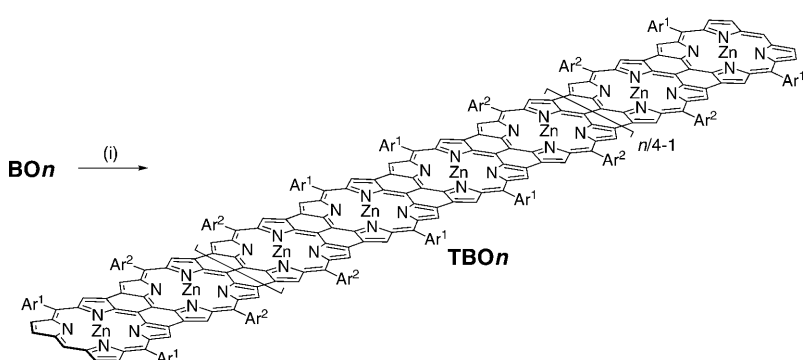


Scheme 4. Ag<sup>I</sup>-promoted oxidation coupling of **BO4**. (i) AgPF<sub>6</sub> (10 equiv), DMA (1 mol %), CH<sub>3</sub>CN, CHCl<sub>3</sub>, reflux, 72 h.

formation). These observations imply that the fractions of 20-mer and 24-mer concomitantly include partially fused parts in their molecular structure. In our previous studies, these partially fused porphyrin arrays were not detected.<sup>[10,16,17]</sup> The formation of such partially fused porphyrin arrays may be ascribed to the rather strong reaction conditions used. Since it is difficult to remove these partially fused oligomers and it does not influence the next fusion reaction of these oligomers, 20-mer and 24-mer were used for the next fusion reaction without further purification.

### Transformation into Porphyrin Tapes

In general, the oxidation of terminal-*meso*-free *meso*-*meso* linked porphyrins with DDQ-Sc(OTf)<sub>3</sub> gives complicated polymeric products as a result of intermolecular coupling. In contrast, the DDQ-Sc(OTf)<sub>3</sub> oxidation of **BOn** in toluene at 80°C for 2 h afforded *meso*-free porphyrin tapes without any intermolecular coupling.<sup>[17]</sup> In this way, terminal-*meso*-free porphyrin tapes **TBOn** were synthesized from **BOn** under the same conditions in the following yields; **TBO4** (63%), **TBO6** (68%), **TBO8** (56%), **TBO12** (52%), **TBO16** (54%), **TBO20** (44%), and **TBO24** (38%) (Scheme 5). The molecular length of the 24-mer reached 20 nm long. MALDI-TOF mass spectroscopy revealed the



Scheme 5. DDQ-Sc(OTf)<sub>3</sub> oxidation of **BOn**. (i) DDQ, Sc(OTf)<sub>3</sub>, toluene, 80°C, 2 h.

parent ion peaks for **TBO4** at *m/z*=5550.21 (calcd for C<sub>360</sub>H<sub>430</sub>N<sub>16</sub>O<sub>20</sub>Zn<sub>4</sub>; *m/z*=5553.03), but the parent ion peaks of higher porphyrin tapes could not be detected by this method. Although the <sup>1</sup>H NMR spectrum of **TBO4** in CDCl<sub>3</sub> showed broadening of peaks, which may be a result of aggregation character, a relatively clear spectrum could be obtained at low concentration (see Supporting Information). The <sup>1</sup>H NMR spectrum shows a singlet for the *meso* proton at 8.24 ppm, a set of mutually coupled doublets for the outer  $\beta$ -protons at 8.06 and 7.99 ppm, and three singlets for the inner  $\beta$ -protons at 7.37, 6.58, and 6.56 ppm. These spectral data are in accord with the previously reported insulated porphyrin tape tetramer.<sup>[17]</sup> The <sup>1</sup>H NMR spectrum of **TBO6** in CDCl<sub>3</sub> displays seriously broadened peaks in the range of 7.8 to 8.5 ppm, which may correspond to the *meso* and  $\beta$  protons. Further assignments of these <sup>1</sup>H NMR spectra were attempted by adding axial ligands, such as *n*-butylamine, using a variety of solvents (C<sub>2</sub>D<sub>2</sub>Cl<sub>4</sub>, [D<sub>5</sub>]pyridine, and [D<sub>8</sub>]toluene), or increasing the temperature; up to 140°C in C<sub>2</sub>D<sub>2</sub>Cl<sub>4</sub>. But these attempts failed owing to the significant aggregation. The observed broadening arises from the  $\pi$ - $\pi$  stacking of porphyrin tapes. Therefore it is conceivable that the regularly introduced bulky aryl groups (Ar<sup>1</sup>) are certainly effective in the suppression of  $\pi$ - $\pi$  stacking for shorter porphyrin tapes but are not sufficient enough for the longer porphyrin tapes. The <sup>1</sup>H NMR spectra of longer porphyrin tapes were quite broad and almost useless for the structural characterizations.

### Optical Properties

The absorption spectra of *meso*-*meso* linked porphyrin oligomers **BOn** in CHCl<sub>3</sub> are shown in Figure 2. Similarly to the previously reported *meso*-*meso* linked porphyrin oligomers,

**BOn** exhibit split Soret bands and red-shifted Q-bands. These split Soret bands can be understood in terms of the exciton coupling theory.<sup>[21,22]</sup> Of the split two Soret bands, the high-energy band remains in the same position as that of a Zn<sup>II</sup> porphyrin monomer, and the other low-energy band is progressively red-shifted as the number of porphyrins increases.

The UV/Vis/NIR absorption spectra of porphyrin tapes **TBOn** in CHCl<sub>3</sub> are shown in

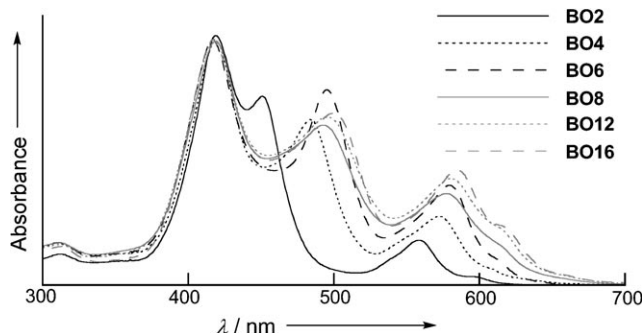


Figure 2. UV/Vis absorption spectra of **BO<sub>n</sub>** in CHCl<sub>3</sub>.

Figure 3. Similarly to the previously reported porphyrin tapes,<sup>[13]</sup> the absorption spectra of **TBO<sub>n</sub>** have three main bands; band I (~400 nm), band II (500~1000 nm), and band

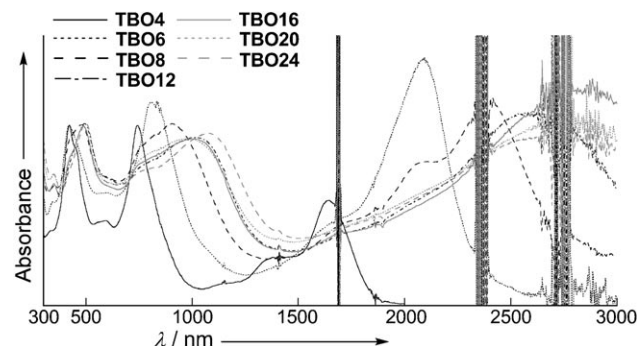


Figure 3. UV/Vis/NIR absorption spectra of **TBO<sub>n</sub>** in CHCl<sub>3</sub>.

III (>1000 nm). Band I is commonly observed around 400 nm at the same position of the Soret band of porphyrins, and band II is shifted to lower energy with an increase in the number of porphyrins, and band III is the lowest energy bands and is most red-shifted with an increase in the number of porphyrins. The bands I and II have been interpreted as split Soret bands and band III has been interpreted as Q-like bands on the basis of several theoretical analyses.<sup>[23]</sup> Band III of **TBO4** and **TBO6** shows typical vibronic structure of porphyrins consisting of Q(0,0) and Q(0,1) absorption bands, and that of **TBO8** partially preserves such vibronic structures. Those of longer oligomers are very broad without such vibronic structure. Importantly, the absorption maxima of band I is observed at 422 nm for **TBO4** and **TBO6**, while that of **TBO8** is observed at 480 nm, and those of the longer porphyrin tapes (**TBO12**, **TBO16**, **TBO20**, and **TBO24**) are observed at 495 nm. These observations may indicate the existence of *J*-aggregate-like aggregations for the longer porphyrin tapes. This interpretation seems in accord with the shapes of band III, considering that aggregation causes the loss of vibronic structure of the porphyrin tape. On the basis of this consideration, it may be concluded that **TBO4** and **TBO6** form no aggregates, **TBO8** partially forms aggregates, and the longer tapes aggregate effectively in CHCl<sub>3</sub>.

Figure 4 shows the plot of the Q(0,1) absorption peak of band III of **TBO<sub>n</sub>** versus the number of porphyrin units *n*. In the previous report,<sup>[16]</sup> it is indicated that the observed

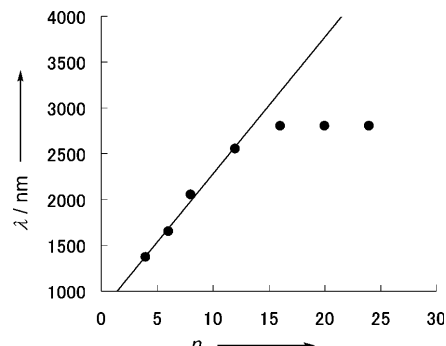


Figure 4. Plots of the Q(0,1) absorption peak of band III of **TBO<sub>n</sub>** from the UV/Vis/NIR spectra versus the number of porphyrin units *n*.

absorption maxima in band III of the broadened absorption spectra of porphyrin tapes is attributed to a Q(0,1) absorption, so the observed peaks in band III of **TBO12**, **TBO16**, **TBO20**, and **TBO24** are Q(0,1) absorptions. In a range of *n* smaller than 12, the plot is linear, but the red-shift of absorption peak is saturated at *n*=16. Because theoretical analysis suggest that the plot would give rise to a well-correlated straight line if the plot was based on the free electron model,<sup>[23a]</sup> saturation of the red-shift means saturation of the extension of  $\pi$ -conjugation, which indicates that the ECL of **TBO<sub>n</sub>** is about 14-mer (ca 12 nm). This is the first experimental observation to reveal the ECL of a triply-linked porphyrin tape.

Since the electronic absorption bands of **TBO<sub>n</sub>** reach the infrared (IR) region, their IR spectra in a KBr pellet were examined (Figure 5). In these spectra, the electronic absorp-

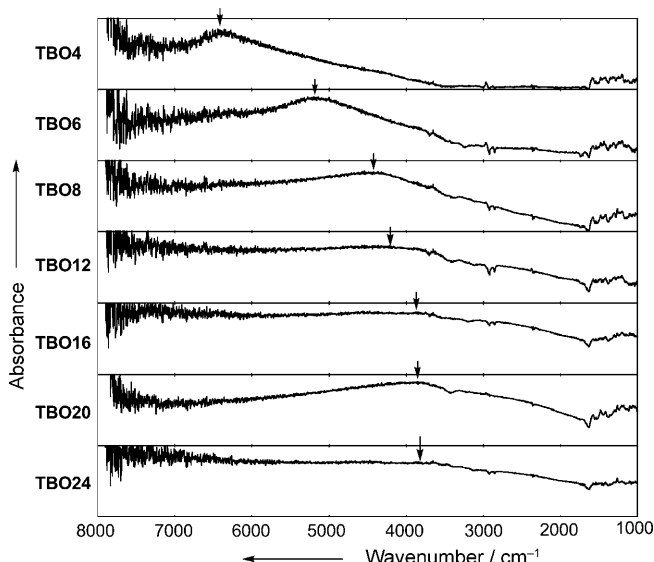


Figure 5. IR absorption spectra of **TBO<sub>n</sub>** in KBr. Arrow indicates the band top position.

tions were actually observed in addition to the stretching and rotational absorptions. Like the UV/Vis/NIR absorption spectra, a red-shift of band III was observed as the number of porphyrin units increases, and the red-shift is saturated at  $3800\text{ cm}^{-1}$  at about  $n=16$ . This result accords with the conclusion obtained from the UV/Vis/NIR spectra.

### Electrochemical Properties

The first oxidation potential of triply linked porphyrin tapes were reported up to the octamer,<sup>[13d]</sup> but details of electrochemical character of porphyrin tapes have not been revealed, mainly owing to the low solubility of porphyrin tapes. The improved solubility of the present porphyrin tapes, caused by the introduction of bulky *meso*-aryl substituents, encourages us to investigate the electrochemical properties of porphyrin tapes. The oxidation and reduction potentials of porphyrin monomer **B1** and porphyrin tapes **TB2**, **TB3**, **TB4**, **TBO4**, **TBO6**, and **TBO8** (for the structures of **TB2**, **TB3**, and **TB4**, see Supporting Information) were measured by cyclic voltammetry (CV) and differential pulse voltammetry (DPV) (Figure S12 in the Supporting Information). Porphyrin tapes showed two reversible peaks for one-electron oxidation and two reversible peaks for one-electron reduction. Unfortunately, the potentials of longer tapes could not be determined because of serious peak broadening. The first oxidation potentials ( $E_{\text{ox}}^1$ ) and the first reduction potentials ( $E_{\text{red}}^1$ ) are summarized in Table 1.  $E_{\text{ox}}^1$  gradually decrease and  $E_{\text{red}}^1$  increase as the number of porphyrin units  $n$  increases. Each of  $E_{\text{ox}}^1$  and  $E_{\text{red}}^1$  are proportional to  $n^{-1}$  (Figure 6a).<sup>[23a]</sup> The reduction potentials of porphyrin tapes were observed for the first time, and the HOMO–LUMO energy gaps were estimated from  $E_{\text{ox}}^1 - E_{\text{red}}^1$  (Table 2), which decrease as  $n$  increases. Table 2 also lists the HOMO–LUMO energy gap estimated by  $\lambda_{\text{max}}$  of band III in the UV/Vis/NIR absorption spectra. These HOMO–LUMO gaps estimated from the electrochemical method and optical method show good agreement and each of them is indirectly proportional to  $n$ . These linear dependencies of oxidation potential, reduction potentials, and also HOMO–LUMO gaps are in line with the view that the electronic delocalization of the porphyrin tapes is fully expanded over the whole array, in which the behaviors of  $\pi$ -electrons are like that of a particle in a box model within ECL (Figure 5b).

Table 1. The oxidation and reduction potentials of porphyrin tapes.

<b>B1<sup>[a]</sup></b>	<b>TB2<sup>[a]</sup></b>	<b>TB3<sup>[a]</sup></b>	<b>TB4<sup>[b]</sup></b>	<b>TBO4<sup>[a]</sup></b>	<b>TBO6<sup>[a]</sup></b>	<b>TBO8<sup>[b]</sup></b>
$E_{\text{ox}}^1 [\text{V}]$	0.37	-0.03	-0.14	-0.27	-0.28	-0.32
$E_{\text{red}}^1 [\text{V}]$	-2.11	-1.21	-0.99	-0.90	-0.88	-0.75
$E_{\text{ox}}^1 - E_{\text{red}}^1 [\text{V}]$	2.48	1.18	0.85	0.63	0.60	0.43

Potentials were measured in anhydrous  $\text{CH}_2\text{Cl}_2$  containing 0.1 M TBABF<sub>4</sub> on Pt working electrode (scan rate: 0.1 V s<sup>-1</sup>). Potential versus Fc/Fc<sup>+</sup>. [a] Potentials were determined by CV. [b] Potentials were determined by DPV.

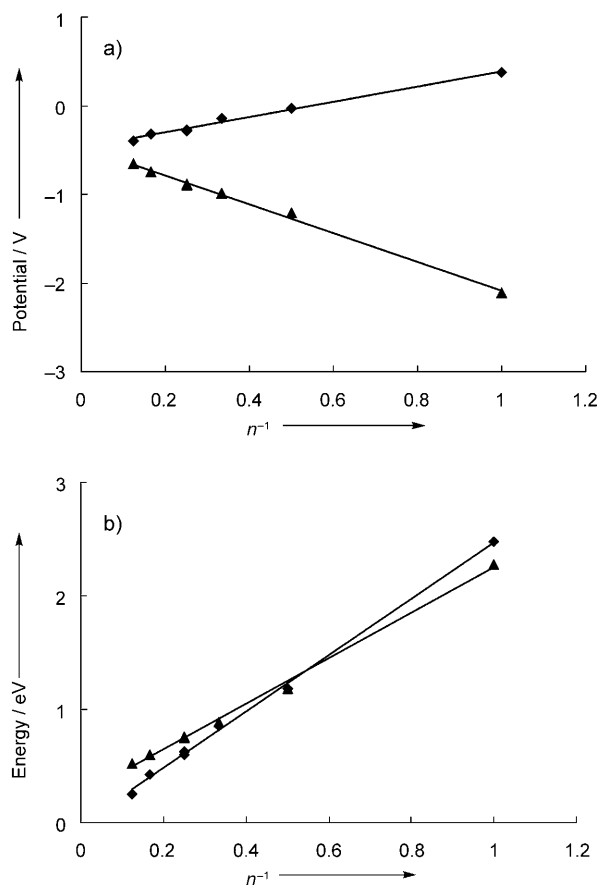


Figure 6. a) The first oxidation potential  $E_{\text{ox}}^1$  (◆) and the first reduction potential  $E_{\text{red}}^1$  (▲) of **B1**, **TB2**, **TB3**, **TB4**, **TBO4**, **TBO6**, and **TBO8** versus the inverse number of porphyrin units  $n$ . b) HOMO–LUMO energy gap estimated by electrochemical method (◆) and optical method (▲) of **B1**, **TB2**, **TB3**, **TB4**, **TBO4**, **TBO6**, and **TBO8** versus the inverse number of porphyrin units  $n$ .

Table 2. HOMO–LUMO energy gap estimated by electrochemical method and optical method.

	<b>B1</b>	<b>TB2</b>	<b>TB3</b>	<b>TB4</b>	<b>TBO4</b>	<b>TBO6</b>	<b>TBO8</b>
electrochemical [eV]	2.48	1.18	0.85	0.63	0.60	0.43	0.25
optical [eV]	2.28	1.18	0.89	0.76	0.75	0.60	0.52

### Summary

Hybrid *meso*-*meso* linked porphyrin arrays and porphyrin tapes, which bear two *meso*-aryl substituents, a bulky group Ar<sup>1</sup> and a non-bulky group Ar<sup>2</sup>, were prepared and characterized. Long porphyrin tape 16-mer, 20-mer, and 24-mer were synthesized for the first time, and the ECL of porphyrin tape was estimated to be about  $n=14$ , which revealed that the porphyrin tape has an extremely extended  $\pi$ -conjugation length

reaching about 12 nm. Additional favorable features are the improved chemical stability and solubility of **TBO<sub>n</sub>** as compared with the conventional porphyrin tapes. From a stability viewpoint, the conventional porphyrin tapes 8-mer and 12-mer were reasonably stable for their separation and manipulations at ambient temperature in air, but bleached slowly during storage in a refrigerator after one or two months. On the other hand, such decompositions were not observed for **TBO<sub>n</sub>** under similar conditions for more than one year, demonstrating that the bulky aryl group improves the chemical stabilities of higher porphyrin tapes. The solubility is also considerably improved, as seen by the nice solubility of **TBO<sub>24</sub>** in CH<sub>2</sub>Cl<sub>2</sub>, CHCl<sub>3</sub>, and toluene, which allow the measurements of the UVVis/NIR absorption spectra in these solvents. These properties are favorable for potential uses of these porphyrin tapes in single molecular spectroscopy and molecular electronics and devices. Efforts along these lines are actively in progress in our laboratory.

## Experimental Section

**Meso-meso linked porphyrin dimer BO2:** 10-Borylated porphyrin **BB1** (100 mg, 53 μmol), 10-brominated porphyrin **BrO1** (67 mg, 64 μmol), Pd<sub>2</sub>(dba)<sub>3</sub> (2.5 mg, 2.6 μmol), PFu<sub>3</sub> (5.0 mg, 10.4 μmol), Cs<sub>2</sub>CO<sub>3</sub> (26 mg, 80 μmol), and CsF (12 mg, 80 μmol) were dissolved in THF/DMF/H<sub>2</sub>O (5.0:1.0:0.1 mL) and the mixture was stirred under N<sub>2</sub> atmosphere at 110°C for 48 h. The resulting mixture was washed with water and brine, dried over Na<sub>2</sub>SO<sub>4</sub>, and evaporated. The residue was passed through a short silica gel column and separated by GPC. Zn insertion was carried out, and further purification by silica gel column chromatography (Wakogel C-400) and recrystallization from CHCl<sub>3</sub>/acetonitrile provided *meso*-*β* linked porphyrin dimer **BO2** as a reddish purple powder. Yield 33 mg (23%). UV/Vis (CHCl<sub>3</sub>):  $\lambda_{\text{max}} (\varepsilon) = 419$  (252000), 451 (190000), and 559 (45300) nm<sup>1</sup>H NMR (600 MHz, CDCl<sub>3</sub>): δ = 0.80 (t,  $J = 6.9$  Hz, 12H, -CH<sub>3</sub>), 0.83 (s, 72H, tBu), 1.20 (s, 36H, tBu), 1.18–1.33 (m, 32H, -CH<sub>2</sub>), 1.43 (m, 8H, -CH<sub>2</sub>), 1.80 (m, 8H, -CH<sub>2</sub>), 4.07 (m, 8H, OCH<sub>2</sub>), 6.48 (m, 8H, Ar-*o*-H), 6.59 (s, 4H, Ar-*m*-H), 6.69 (m, 4H, Ar-*o*-H), 6.81 (m, 2H, Ar-*p*-H), 6.96 (m, 4H, Ar-*p*-H), 7.10 (m, 2H, Ar-*p*-H), 7.42 (m, 4H, Ar-*o*-H), 8.07 (d,  $J = 4.1$  Hz, 2H, β), 8.09 (br, 2H, β), 8.73 (d,  $J = 4.1$  Hz, 2H, β), 8.95 (d,  $J = 4.1$  Hz, 2H, β), 9.27 (d,  $J = 4.1$  Hz, 2H, β), 9.44 (d,  $J = 4.1$  Hz, 2H, β), 9.47 (d,  $J = 4.1$  Hz, 2H, β), 9.50 (d,  $J = 4.1$  Hz, 2H, β), 10.23 (s, 1H, *meso*), and 10.39 ppm (s, 1H, *meso*); MS (MALDI-TOF): found  $m/z = 2786.68$ , calcd for C<sub>180</sub>H<sub>224</sub>N<sub>8</sub>O<sub>10</sub>Zn<sub>2</sub>,  $m/z = 2788.51$ .

**Meso-meso linked porphyrin tetramer BO4:** *Meso-meso* linked dimer **BO2** (200 mg, 72 μmol) was dissolved in dry chloroform (70 mL). To the solution was added a stock solution of AgPF<sub>6</sub> in acetonitrile (0.12 M, 3.0 mL, 360 μmol) under N<sub>2</sub> atmosphere in the dark and the reaction mixture was stirred at room temperature for 12 h and the reaction was quenched by addition of water. The organic layer was separated, washed with brine, dried over Na<sub>2</sub>SO<sub>4</sub>, and evaporated. Zn insertion was carried out, and the residue was passed through a short silica gel column and separated by GPC. Further purification by silica gel column chromatography (Wakogel C-400) and recrystallization from CHCl<sub>3</sub>/acetonitrile provided *meso-meso* linked tetramer **BO4** (70 mg, 35%) along with hexamer **BO6** (1.0 mg, 0.5%) and starting material **BO2** (112 mg, 56%). **BO4:** UV/Vis (CHCl<sub>3</sub>):  $\lambda_{\text{max}} (\varepsilon) = 419$  (430000), 484 (290000), and 572 (121000) nm; <sup>1</sup>H NMR (600 MHz, CDCl<sub>3</sub>): δ = 0.75 (t,  $J = 6.9$  Hz, 24H, -CH<sub>3</sub>), 0.87 (s, 144H, tBu), 1.23 (s, 72H, tBu), 1.14–1.32 (m, 64H, -CH<sub>2</sub>), 1.39 (m, 16H, -CH<sub>2</sub>), 1.77 (m, 16H, -CH<sub>2</sub>), 4.01 (m, 16H, OCH<sub>2</sub>), 6.53 (m, 16H, Ar-*o*-H), 6.64 (s, 8H, Ar-*m*-H), 6.71 (m, 8H, Ar-*o*-H), 6.72 (m, 4H, Ar-*p*-H), 6.99 (m, 8H, Ar-*p*-H), 7.13 (m, 4H, Ar-*p*-H), 7.45 (m, 8H, Ar-*o*-H), 8.13 (br, 4H, β), 8.24 (d,  $J = 4.1$  Hz, 4H, β), 8.33 (d,  $J = 4.1$  Hz, 4H, β), 8.76 (d,  $J = 4.1$  Hz, 4H, β), 8.89 (d,  $J = 4.1$  Hz, 4H, β), 9.04 (d,  $J = 4.1$  Hz, 4H, β), 9.45 (d,  $J = 4.1$  Hz, 4H, β), 9.49 (d,  $J = 4.1$  Hz, 4H, β), and

10.23 ppm (s, 2H, *meso*); MS (MALDI-TOF): found  $m/z = 5573.11$ , calcd for C<sub>360</sub>H<sub>442</sub>N<sub>16</sub>O<sub>20</sub>Zn<sub>4</sub>,  $m/z = 5575.00$ . **BO6:** UV/Vis (CHCl<sub>3</sub>):  $\lambda_{\text{max}} (\varepsilon) = 417$  (529000), 495 (422000), and 579 (216000) nm; <sup>1</sup>H NMR (600 MHz, CDCl<sub>3</sub>): δ = 0.77 (m, 36H, -CH<sub>3</sub>), 0.82 (s, 72H, tBu), 0.88 (s, 72H, tBu), 0.89 (s, 72H, tBu), 1.17 (s, 36H, tBu), 1.25 (m, 72H, tBu), 1.14–1.32 (m, 96H, -CH<sub>2</sub>), 1.40 (m, 24H, -CH<sub>2</sub>), 1.77 (m, 24H, -CH<sub>2</sub>), 4.05 (m, 24H, OCH<sub>2</sub>), 6.54 (m, 8H, Ar-*o*-H), 6.55 (m, 8H, Ar-*o*-H), 6.61 (s, 4H, Ar-*m*-H), 6.65 (s, 4H, Ar-*m*-H), 6.66 (s, 4H, Ar-*m*-H), 6.73 (m, 12H, Ar-*o*-H), 6.75 (m, 4H, Ar-*p*-H), 6.78 (m, 2H, Ar-*p*-H), 6.94 (m, 4H, Ar-*p*-H), 7.02 (m, 8H, Ar-*p*-H), 7.08 (m, 2H, Ar-*p*-H), 7.14 (m, 4H, Ar-*p*-H), 7.47 (m, 8H, Ar-*o*-H), 7.51 (m, 4H, Ar-*o*-H), 8.17 (br, 4H, β), 8.31–8.38 (m, 16H, β), 8.78 (m, 4H, β), 8.85 (d,  $J = 4.1$  Hz, 2H, β), 8.87 (d,  $J = 4.1$  Hz, 2H, β), 8.93 (d,  $J = 4.1$  Hz, 2H, β), 8.95 (d,  $J = 4.1$  Hz, 2H, β), 9.06 (m, 4H, β), 9.11 (m, 4H, β), 9.48 (m, 4H, β), 9.51 (m, 4H, β), and 10.26 ppm (m, 2H, *meso*); MS (MALDI-TOF): found  $m/z = 8349.28$ , calcd for C<sub>540</sub>H<sub>660</sub>N<sub>24</sub>O<sub>30</sub>Zn<sub>6</sub>,  $m/z = 8359.48$ .

**Meso-meso linked porphyrin oligomers BO<sub>n</sub>:** *Meso-meso* linked tetramer **BO4** (150 mg, 27 μmol) was dissolved in dry chloroform (27 mL). To the solution was added a stock solution of AgPF<sub>6</sub> in acetonitrile (0.12 M, 1.1 mL, 134 μmol) and N,N-dimethylacetamide (DMA, 27 μL, 0.27 μmol) under N<sub>2</sub> atmosphere in the dark and the reaction mixture was stirred under reflux for 72 h and the reaction was quenched by addition of water. The organic layer was separated, washed with brine, dried over Na<sub>2</sub>SO<sub>4</sub>, and evaporated. Zn insertion was carried out, and the residue was passed through a short silica gel column and separated by GPC. Further purification by silica gel column chromatography (Wakogel C-400) and recrystallization from CHCl<sub>3</sub>/acetonitrile provided *meso-meso* linked oligomers **BO8** (15%), **BO12** (5%), **BO16** (2%), 20-mer (1%), 24-mer (0.6%), and recovered **BO4** (51%). **BO8:** UV/Vis (CHCl<sub>3</sub>):  $\lambda_{\text{max}} (\varepsilon) = 419$  (669000), 492 (438000), and 578 (251000) nm; <sup>1</sup>H NMR (600 MHz, CDCl<sub>3</sub>): δ = 0.77 (m, 48H, -CH<sub>3</sub>), 0.82 (s, 144H, tBu), 0.88 (s, 144H, tBu), 1.18 (s, 72H, tBu), 1.25 (s, 72H, tBu), 1.14–1.32 (m, 128H, -CH<sub>2</sub>), 1.40 (m, 32H, -CH<sub>2</sub>), 1.77 (m, 32H, -CH<sub>2</sub>), 4.05 (m, 32H, OCH<sub>2</sub>), 6.55 (m, 32H, Ar-*o*-H), 6.66 (s, 16H, Ar-*m*-H), 6.73 (m, 8H, Ar-*o*-H), 6.75 (m, 8H, Ar-*o*-H), 6.78 (m, 8H, Ar-*p*-H), 6.95 (m, 8H, Ar-*p*-H), 7.01 (m, 8H, Ar-*p*-H), 7.08 (m, 4H, Ar-*p*-H), 7.14 (m, 4H, Ar-*p*-H), 7.47 (m, 8H, Ar-*o*-H), 7.51 (m, 8H, Ar-*o*-H), 8.16 (br, 4H, β), 8.31–8.40 (m, 20H, β), 8.78 (m, 4H, β), 8.85 (d,  $J = 4.1$  Hz, 2H, β), 8.92–8.96 (m, 8H, β), 9.04–9.11 (m, 8H, β), 9.48 (m, 4H, β), 9.51 (m, 4H, β), and 10.26 ppm (s, 2H, *meso*); MS (MALDI-TOF): found  $m/z = 11142.87$ , calcd for C<sub>720</sub>H<sub>882</sub>N<sub>32</sub>O<sub>40</sub>Zn<sub>8</sub>,  $m/z = 11147.98$ . **BO12:** UV/Vis (CHCl<sub>3</sub>):  $\lambda_{\text{max}} (\varepsilon) = 418$  (919000), 495 (628000), and 580 (399000) nm; <sup>1</sup>H NMR (600 MHz, CDCl<sub>3</sub>): δ = 0.77 (m, 72H, -CH<sub>3</sub>), 0.82 (s, 144H, tBu), 0.88 (s, 288H, tBu), 1.18 (s, 72H, tBu), 1.25 (s, 144H, tBu), 1.14–1.32 (m, 192H, -CH<sub>2</sub>), 1.40 (m, 48H, -CH<sub>2</sub>), 1.77 (m, 48H, -CH<sub>2</sub>), 4.05 (m, 48H, OCH<sub>2</sub>), 6.55 (m, 48H, Ar-*o*-H), 6.67 (m, 24H, Ar-*m*-H), 6.73 (m, 8H, Ar-*o*-H), 6.75 (m, 16H, Ar-*o*-H), 6.80 (m, 12H, Ar-*p*-H), 6.96 (m, 16H, Ar-*p*-H), 7.02 (m, 8H, Ar-*p*-H), 7.09 (m, 8H, Ar-*p*-H), 7.14 (m, 4H, Ar-*p*-H), 7.48 (m, 8H, Ar-*o*-H), 7.51 (m, 16H, Ar-*o*-H), 8.16 (br, 4H, β), 8.31–8.40 (m, 32H, β), 8.78 (m, 4H, β), 8.85–9.01 (m, 16H, β), 9.04–9.11 (m, 16H, β), 9.48 (m, 4H, β), 9.51 (m, 4H, β), and 10.26 ppm (s, 2H, *meso*); MS (MALDI-TOF): found  $m/z = 16712.89$ , calcd for C<sub>1080</sub>H<sub>1222</sub>N<sub>48</sub>O<sub>60</sub>Zn<sub>12</sub>,  $m/z = 16720.97$ . **BO16:** UV/Vis (CHCl<sub>3</sub>):  $\lambda_{\text{max}} (\varepsilon) = 417$  (1110000), 500 (776000), and 585 (518000) nm; <sup>1</sup>H NMR (600 MHz, CDCl<sub>3</sub>): δ = 0.77 (m, 96H, -CH<sub>3</sub>), 0.82 (s, 144H, tBu), 0.88 (s, 432H, tBu), 1.18 (s, 72H, tBu), 1.25 (s, 216H, tBu), 1.14–1.32 (m, 256H, -CH<sub>2</sub>), 1.40 (m, 64H, -CH<sub>2</sub>), 1.77 (m, 64H, -CH<sub>2</sub>), 4.05 (m, 64H, OCH<sub>2</sub>), 6.55 (m, 64H, Ar-*o*-H), 6.67 (m, 32H, Ar-*m*-H), 6.73 (m, 8H, Ar-*o*-H), 6.75 (m, 24H, Ar-*o*-H), 6.80 (m, 16H, Ar-*p*-H), 6.96 (m, 24H, Ar-*p*-H), 7.02 (m, 8H, Ar-*p*-H), 7.09 (m, 12H, Ar-*p*-H), 7.14 (m, 4H, Ar-*p*-H), 7.48 (m, 8H, Ar-*o*-H), 7.51 (m, 24H, Ar-*o*-H), 8.16 (br, 4H, β), 8.31–8.40 (m, 56H, β), 8.78 (m, 4H, β), 8.85–9.01 (m, 28H, β), 9.04–9.11 (m, 28H, β), 9.48 (m, 4H, β), 9.51 (m, 4H, β), and 10.26 ppm (s, 2H, *meso*); MS (MALDI-TOF): found  $m/z = 22279.91$ , calcd for C<sub>1440</sub>H<sub>1762</sub>N<sub>64</sub>O<sub>80</sub>Zn<sub>16</sub>,  $m/z = 22293.94$ . **20-mer:** MS (MALDI-TOF): found  $m/z = 27848.75$ , calcd for C<sub>1800</sub>H<sub>2202</sub>N<sub>80</sub>O<sub>100</sub>Zn<sub>20</sub> (**BO20**),  $m/z = 27866.22$ . **24-mer:** MS (MALDI-TOF): found  $m/z = 33215.24$ , calcd for C<sub>2160</sub>H<sub>2442</sub>N<sub>96</sub>O<sub>120</sub>Zn<sub>24</sub> (**BO24**),  $m/z = 33237.46$ .

**General procedure for DDQ-Sc(OTf)<sub>3</sub> oxidation.** To a solution of *meso*-*meso* linked porphyrin array (10 mg) in dry toluene (10 mL) was added 4-(*n*-1) equivalent of DDQ and 4(*n*-1) equivalent of Sc(OTf)<sub>3</sub>. The resulting reaction mixture was stirred at 80°C for 2 h under N<sub>2</sub> atmosphere in the dark and the reaction was quenched by the addition of THF. The resulting mixture was passed through a short alumina column and the solvent was evaporated. Further purification by silica gel column chromatography (Wakogel C-400) and recrystallization from CHCl<sub>3</sub>/acetonitrile provided triply linked porphyrin tape.

**Porphyrin tape tetramer TBO4:** Following the general procedure, **TBO4** was prepared from **BO4** in 63% yield as green solids. MS (MALDI-TOF): found *m/z*=5550.21, calcd for C<sub>360</sub>H<sub>430</sub>N<sub>16</sub>O<sub>20</sub>Zn<sub>4</sub>; *m/z*=5553.03; UV/Vis (CHCl<sub>3</sub>):  $\lambda_{\text{max}}$ =423, 744, 1401, and 1646 nm.

**Porphyrin tape hexamer TBO6:** Following the general procedure, **TBO6** was prepared from **BO6** in 68% yield as black solids. UV/Vis (CHCl<sub>3</sub>):  $\lambda_{\text{max}}$ =422, 598, and 2110 nm.

**Porphyrin tape octamer TBO8:** Following the general procedure, **TBO8** was prepared from **BO8** in 56% yield as black solids. UV/Vis (CHCl<sub>3</sub>):  $\lambda_{\text{max}}$ =480, 910, 2108, and 2410 nm.

**Porphyrin tape dodecamer TBO12:** Following the general procedure, **TBO12** was prepared from **BO12** in 52% yield as black solids. UV/Vis (CHCl<sub>3</sub>):  $\lambda_{\text{max}}$ =494, 1018, and 2580 nm.

**Porphyrin tape hexadecamer TBO16:** Following the general procedure, **TBO16** was prepared from **BO16** in 54% yield as black solids. UV/Vis (CHCl<sub>3</sub>):  $\lambda_{\text{max}}$ =490, 1008, and 2800 nm.

**Porphyrin tape icosamer TBO20:** Following the general procedure, **TBO20** was prepared from **BO20** in 44% yield as black solids. UV/Vis (CHCl<sub>3</sub>):  $\lambda_{\text{max}}$ =490, 982, and 2800 nm.

**Porphyrin tape tetracosamer TBO24:** Following the general procedure, **TBO24** was prepared from **BO24** in 38% yield as black solids. UV/Vis (CHCl<sub>3</sub>):  $\lambda_{\text{max}}$ =500, 1072, and 2800 nm.

## Acknowledgements

The work was supported by Grants-in-Aid for Scientific Research (No. 19205006, and 20108001 “pi-Space”) from the Ministry of Education, Culture, Sports, Science and Technology, Japan. N.A. thanks a Grant-in-Aid for Young Scientists (B) and GCOE program “Integrated Materials Science” for financial support. T.I. thanks the JSPS Research fellowships for Young Scientists.

- [1] a) R. E. Martin, F. Diederich, *Angew. Chem.* **1999**, *111*, 1440–1469; *Angew. Chem. Int. Ed.* **1999**, *38*, 1350–1377; b) J. M. Tour, *Chem. Rev.* **1996**, *96*, 537–554; c) P. F. H. Schwab, M. D. Levin, J. Michl, *Chem. Rev.* **1999**, *99*, 1863–1934; d) J. Cornil, D. Beljonne, J.-P. Cabbert, J.-L. Brédas, *Adv. Mater.* **2001**, *13*, 1053–1067; e) A. Kraft, A. C. Grimsdale, A. B. Holmes, *Angew. Chem.* **1998**, *110*, 416–443; *Angew. Chem. Int. Ed.* **1998**, *37*, 402–428; f) J. S. Moore, *Acc. Chem. Res.* **1997**, *30*, 402–413; g) D. T. McQuade, A. E. Pullen, T. M. Swager, *Chem. Rev.* **2000**, *100*, 2537–2574; h) U. H. F. Bunz, *Chem. Rev.* **2000**, *100*, 1605–1644; i) M. D. Watson, A. Fechtenkötter, K. Müllen, *Chem. Rev.* **2001**, *101*, 1267–1300; j) F. Diederich, *Chem. Commun.* **2001**, 219–227.
- [2] a) P. Liess, V. Hensel, A. D. Schlüter, *Liebigs Ann.* **1996**, 1037–1040; b) U. Stalmach, H. Kolhorn, I. Brehm, H. Meier, *Liebigs Ann.* **1996**, 1449–1456; c) R. E. Martin, U. Gubler, J. Cornil, M. Balakina, C. Boudon, C. Bossard, J.-P. Gisselbrecht, F. Diederich, P. Günther, M. Gross, J.-L. Brédas, *Chem. Eur. J.* **2000**, *6*, 3622–3635; d) N. Sumi, H. Nakanishi, S. Ueno, K. Takimiya, Y. Aso, T. Otsubo, *Bull. Chem. Soc. Jpn.* **2001**, *74*, 979–988; e) T. Izumi, S. Kobashi, K. Takimiya, Y. Aso, T. Otsubo, *J. Am. Chem. Soc.* **2003**, *125*, 5286–5287; f) T. Gibtner, F. Hampel, J.-P. Gisselbrecht, A. Hirsch, *Chem. Eur. J.* **2002**, *8*, 408–432; g) L. Dunsch, P. Rapta, N. Schulte, A. D. Schlüter, *Angew. Chem.* **2002**, *114*, 2187–2190; *Angew. Chem. Int. Ed.* **2002**, *41*, 2082–2086; h) S. Toyota, M. Goichi, M. Kotani, *Angew. Chem.* **2004**, *116*, 2298–2301; *Angew. Chem. Int. Ed.* **2004**, *43*, 2248–2251; i) W.-S. Li, D.-L. Jiang, T. Aida, *Angew. Chem.* **2004**, *116*, 3003–3007; *Angew. Chem. Int. Ed.* **2004**, *43*, 2943–2947; j) Q. Zheng, J. A. Gladysz, *J. Am. Chem. Soc.* **2005**, *127*, 10508–10509.
- [3] a) H. Meier, *Angew. Chem.* **2005**, *117*, 2536–2561; *Angew. Chem. Int. Ed.* **2005**, *44*, 2482–2506; b) E. Clar, *Ber. Dtsch. Chem. Ges.* **1936**, *69*, 607–614; c) H. Meier, U. Stalmach, H. Kolhorn, *Acta Polym.* **1997**, *48*, 379–384; d) S. Eisler, A. D. Slepov, E. Elliott, T. Luu, R. McDonald, F. A. Hegmann, R. R. Tykwinski, *J. Am. Chem. Soc.* **2005**, *127*, 2666–2676; T. Luu, R. McDonald, F. A. Hegmann, R. R. Tykwinski, *J. Am. Chem. Soc.* **2005**, *127*, 2666–2676.
- [4] J. H. Chou, H. S. Nalwa, M. E. Kosai, N. A. Rakow, K. S. Suslick, *The Porphyrin Handbook, Vol. 6* (Eds.: K. M. Kadish, K. M. Smith, R. Guilard), Academic Press, San Diego, **2000**, Chap. 41.
- [5] a) N. Ono, H. Hironaga, K. Ono, S. Kaneko, T. Murashima, T. Ueda, C. Tsukamura, T. Ogawa, *J. Chem. Soc. Perkin Trans. 1* **1996**, 417–423; b) S. Ito, T. Murashima, N. Ono, H. Uno, *Chem. Commun.* **1998**, 1661–1662; c) H. Uno, A. Masumoto, N. Ono, *J. Am. Chem. Soc.* **2003**, *125*, 12082–12083; d) O. S. Finikova, A. V. Cheprakov, I. P. Beletskaya, P. J. Carroll, S. A. Vinogradov, *J. Org. Chem.* **2004**, *69*, 522–535; e) K. Sugiyama, T. Matsumoto, S. Ohkouchi, Y. Naitoh, T. Kawai, Y. Takai, K. Ushiroda, Y. Sakata, *Chem. Commun.* **1999**, 1957–1958; f) O. Yamane, K. Sugiyama, H. Miyasaka, K. Nakamura, T. Fujimoto, K. Nakamura, T. Kaneda, Y. Sakata, M. Yamashita, *Chem. Lett.* **2004**, *33*, 40–41; g) A. N. Cammidge, P. J. Scaife, G. Berber, D. L. Hughes, *Org. Lett.* **2005**, *7*, 3413–3416; h) T. D. Lash, P. Chandrasekar, *J. Am. Chem. Soc.* **1996**, *118*, 8767–8768; i) T. D. Lash, S. T. Chaney, *Angew. Chem.* **1997**, *109*, 867–868; *Angew. Chem. Int. Ed. Engl.* **1997**, *36*, 839–840.
- [6] a) D. P. Arnold, A. W. Johnson, M. Mahendran, *J. Chem. Soc. Perkin Trans. 1* **1978**, 366–370; b) D. P. Arnold, G. A. Heath, *J. Am. Chem. Soc.* **1993**, *115*, 12197–12198.
- [7] a) V. S. Y. Lin, S. G. DiMaggio, M. J. Therien, *Science* **1994**, 264, 1105–1111; b) S. M. LeCours, H.-W. Guan, S. G. DiMaggio, C. H. Wang, M. J. Therien, *J. Am. Chem. Soc.* **1996**, *118*, 1497–1503; c) H. T. Uyeda, Y. Zhao, K. Wostyn, I. Asselberghs, K. Clays, A. Persoons, M. J. Therien, *J. Am. Chem. Soc.* **2002**, *124*, 13806–13813; d) K. Susumu, T. V. Duncan, M. J. Therien, *J. Am. Chem. Soc.* **2005**, *127*, 5186–5195.
- [8] a) H. L. Anderson, *Chem. Commun.* **1999**, 2323–2330; b) P. N. Taylor, A. P. Wylie, J. Huusonen, H. L. Anderson, *Angew. Chem.* **1998**, *110*, 1033–1037; *Angew. Chem. Int. Ed.* **1998**, *37*, 986–989; c) I. M. Blake, H. L. Anderson, D. Beljonne, J.-L. Brédas, W. Clegg, *J. Am. Chem. Soc.* **1998**, *120*, 10764–10765; d) I. M. Blake, L. H. Rees, T. D. W. Claridge, H. L. Anderson, *Angew. Chem.* **2000**, *112*, 1888–1891; *Angew. Chem. Int. Ed.* **2000**, *39*, 1818–1821.
- [9] J. Wytko, V. Berl, M. McLaughlin, R. R. Tykwinski, M. Schreiber, F. Diederich, C. Boudon, J. P. Gisselbrecht, W. E. Jones, *Helv. Chim. Acta* **1998**, *81*, 1964–1977.
- [10] a) A. Osuka, H. Shimidzu, *Angew. Chem.* **1997**, *109*, 93–95; *Angew. Chem. Int. Ed. Engl.* **1997**, *36*, 135–137; b) A. Nakano, A. Osuka, I. Yamazaki, T. Yamazaki, Y. Nishimura, *Angew. Chem.* **1998**, *110*, 3172–3176; *Angew. Chem. Int. Ed.* **1998**, *37*, 3023–3027; c) N. Aratani, A. Osuka, Y. H. Kim, D. H. Jeong, D. Kim, *Angew. Chem.* **2000**, *112*, 1517–1521; *Angew. Chem. Int. Ed.* **2000**, *39*, 1458–1462; d) A. Nakano, T. Yamazaki, Y. Nishimura, I. Yamazaki, A. Osuka, *Chem. Eur. J.* **2000**, *6*, 3254–3271; e) N. Aratani, A. Takagi, Y. Yanagawa, T. Matsumoto, T. Kawai, Z. S. Yoon, D. Kim, A. Osuka, *Chem. Eur. J.* **2005**, *11*, 3389–3404.
- [11] a) M. J. Crossley, P. L. Burn, *J. Chem. Soc. Chem. Commun.* **1991**, 1569–1571; b) K. Sendt, L. A. Johnston, W. A. Hough, M. J. Crossley, N. S. Hush, J. R. Reimers, *J. Am. Chem. Soc.* **2002**, *124*, 9299–9309.
- [12] a) M. G. H. Vicente, L. Jaquinod, K. M. Smith, *Chem. Commun.* **1999**, 1771–1782; b) L. Jaquinod, O. Siri, R. G. Khoury, K. M. Smith, *Chem. Commun.* **1998**, 1261–1262; c) M. G. H. Vicente, M. T. Cancilla, C. B. Lebrilla, K. M. Smith, *Chem. Commun.* **1998**, 2355–2356; d) R. Paolese, L. Jaquinod, F. D. Sala, D. J. Nurco, L.

- Prodi, M. Montalti, C. D. Natale, A. D'Amico, A. D. Carlo, P. Lugli, K. M. Smith, *J. Am. Chem. Soc.* **2000**, *122*, 11295–11302; e) H. Aihara, L. Jaquinod, D. J. Nurco, K. M. Smith, *Angew. Chem.* **2001**, *113*, 3547–3549; *Angew. Chem. Int. Ed.* **2001**, *40*, 3439–3441; f) M. Nath, J. C. Huffman, J. M. Zaleski, *J. Am. Chem. Soc.* **2003**, *125*, 11484–11485.
- [13] a) A. Tsuda, A. Nakano, H. Furuta, H. Yamochi, A. Osuka, *Angew. Chem.* **2000**, *112*, 572–575; *Angew. Chem. Int. Ed.* **2000**, *39*, 558–561; b) A. Tsuda, H. Furuta, A. Osuka, *Angew. Chem.* **2000**, *112*, 2649–2652; *Angew. Chem. Int. Ed.* **2000**, *39*, 2549–2552; c) A. Tsuda, H. Furuta, A. Osuka, *J. Am. Chem. Soc.* **2001**, *123*, 10304–10321; d) A. Tsuda, A. Osuka, *Science* **2001**, *293*, 79–82; e) S. Hiroto, A. Osuka, *J. Org. Chem.* **2005**, *70*, 4054–4058; f) T. Ikeue, N. Aratani, A. Osuka, *Isr. J. Chem.* **2005**, *45*, 293–302.
- [14] a) A. Tsuda, Y. Nakamura, A. Osuka, *Chem. Commun.* **2003**, 1096–1097; b) M.-C. Yoon, S. B. Noh, A. Tsuda, Y. Nakamura, A. Osuka, D. Kim, *J. Am. Chem. Soc.* **2007**, *129*, 10080–10081.
- [15] a) T. K. Ahn, K. S. Kim, D. Y. Kim, S. B. Noh, N. Aratani, C. Ikeda, A. Osuka, D. Kim, *J. Am. Chem. Soc.* **2006**, *128*, 1700–1704; b) D. H. Yoon, S. B. Lee, K.-H. Yoo, J. Kim, J. K. Lim, N. Aratani, A. Tsuda, A. Osuka, D. Kim, *J. Am. Chem. Soc.* **2003**, *125*, 11062–11064; c) Y. Nakamura, S. Y. Jang, T. Tanaka, N. Aratani, J. M. Lim, K. S. Kim, D. Kim, A. Osuka, *Chem. Eur. J.* **2008**, *14*, 8279–8289.
- [16] T. Ikeda, J. M. Lintuluoto, N. Aratani, Z. S. Yoon, D. Kim, A. Osuka, *Eur. J. Org. Chem.* **2006**, 3193–3204.
- [17] T. Ikeda, A. Tsuda, N. Aratani, A. Osuka, *Chem. Lett.* **2006**, *35*, 946–947.
- [18] A. G. Hyslop, M. A. Kellett, P. M. Iovine, M. J. Therien, *J. Am. Chem. Soc.* **1998**, *120*, 12676–12677.
- [19] N. Aratani, A. Osuka, *Org. Lett.* **2001**, *3*, 4213–4216.
- [20] N. Yoshida, N. Aratani, A. Osuka, *Chem. Commun.* **2000**, 197–198.
- [21] M. Kasha, *Radiat. Res.* **1963**, *20*, 55–70.
- [22] a) Y. H. Kim, D. H. Jeong, D. Kim, S. C. Jeoung, H. S. Cho, S. K. Kim, N. Aratani, A. Osuka, *J. Am. Chem. Soc.* **2001**, *123*, 76–86; b) D. H. Jeong, S. M. Jang, I.-W. Hwang, D. Kim, N. Yoshida, A. Osuka, *J. Phys. Chem. A* **2002**, *106*, 11054–11063; c) N. Yoshida, T. Ishizuka, A. Osuka, D. H. Jeong, H. S. Cho, D. Kim, Y. Matsuzaki, A. Nogami, K. Tanaka, *Chem. Eur. J.* **2003**, *9*, 58–75.
- [23] a) H. S. Cho, D. H. Jeong, S. Cho, D. Kim, Y. Matsuzaki, K. Tanaka, A. Tsuda, A. Osuka, *J. Am. Chem. Soc.* **2002**, *124*, 14642–14654; b) T. Miyahara, H. Nakatsuji, J. Hasegawa, A. Osuka, N. Aratani, A. Tsuda, *J. Chem. Phys.* **2002**, *117*, 11196–11207.

Received: April 2, 2009

Published online: June 30, 2009